

# Characterization and identification of leaf-scale wheat powdery mildew using a ground-based hyperspectral imaging system

Jinling Zhao<sup>1,2</sup>, Wenjiang Huang<sup>1\*</sup>, Dongyan Zhang<sup>1</sup>, Juhua Luo<sup>1</sup>, Jingcheng Zhang<sup>1</sup>, Linsheng Huang<sup>1</sup> and Shilin Chen<sup>3</sup>

1. Beijing Research Center for Information Technology in Agriculture, Beijing 100097, CHINA

2. Institute of Remote Sensing Applications, Chinese Academy of Sciences, Beijing 100101, CHINA

3. Xinjiang Vocational and Technical College, Urumqi, 830000, CHINA

\*yellowstar0618@163.com

## Abstract

The objective of this study is to characterize and identify wheat leaves infected with powdery mildew using a domestic-made ground-based hyperspectral push-broom imaging spectrometer (PIS) with a spectral resolution of 2 nm and a spatial resolution of 5-10 nm. After performing a data preprocessing including image mosaicing, reflectance conversion and spectral smoothing, the image and spectral characteristics were investigated based on the high spatial and spectral resolution hyperspectral data cube acquired by this system. To explore the image characteristics, occurrence-based texture filters were utilized and their combination of data range, mean, variance were proved to be effective in differentiating disease spots from normal leaves. On the basis of identifying characteristic bands (10 red bands (675.1-681.1 nm) and 10 near-infrared bands (706.2-712.1 nm) were respectively averaged) sensitive to this disease, an image feature space (X axis: red; Y axis: NIR) was built to identify disease spots by a linear regression model ( $y=3.48*x-7.57$ ) which was constructed using a total of 220 pixels from normal leaf and disease spot. To validate the identification accuracy of the model, 120 pixels were used and the overall classification accuracy reached 92.5%. The misclassification was caused due to nonuniform lighting in the process of scanning. Final identification results indicated that corresponding texture and spectral information were greatly enhanced due to the influence of pustular spots of powdery mildew. The analysis results demonstrated that it was feasible to identify disease spots of powdery mildew using the PIS.

**Keywords:** Powdery Mildew, Leaf-Scale Wheat, Hyperspectral Imaging System, Texture Analysis.

## Introduction

Powdery mildew (*Blumeria graminis* f. sp. *tritici*) is one of primary fungal diseases in common wheat (*Triticum aestivum* L.) worldwide, which has caused significant yield and quality losses<sup>1-3</sup>. It is an important biological disaster to hinder a sustainable development in precision agriculture to a certain degree. Improving the ability of identifying diseases

in an early infestation stage is crucial for farmers to aid in agricultural decision making<sup>4,6</sup>. Consequently, it is of significant importance to understand the disease symptoms and quantify infestation severity. However, traditional methods of disease assessment rely heavily on on-farm investigations and unfortunately the observations from field surveys can only reflect the disease severity within a relatively small radius<sup>7</sup>.

In recent years, the development of remote sensing has been identified as an effective tool to nondestructively monitor wheat diseases at a large spatial scale<sup>8</sup>. For example, Franke and Menz examined the potential of multi-spectral high resolution remote sensing for a multi-temporal analysis of wheat powdery mildew (*Blumeria graminis*) and leaf rust (*Puccinia recondita*) pathogens<sup>9</sup>. Chen *et al.* detected the severe infestation of the take-all disease in wheat using two-period Landsat Thematic Mapper (TM) imageries<sup>10</sup>. Li *et al.* used hyperspectral indices from an ASD (Analytical Spectral Devices) FieldSpec Pro FR<sup>TM</sup> spectrometer in the field to estimate foliar chlorophyll concentrations of winter wheat under yellow rust stress<sup>11</sup>. Mewes *et al.* investigated wheat stands infected with powdery mildew using a single airborne hyperspectral HyMap dataset<sup>12</sup>. To summarize the above studies, it can be found that three types of remotely sensed data have been extensively utilized from spaceborne, airborne and near-ground hyperspectral sensors. In comparison with multispectral images with wide wavebands, hyperspectral datasets with hundreds of narrow bands can provide more detailed information on wheat diseases in specific visible, near- and middle-infrared regions of electromagnetic spectrum<sup>13</sup>. Therefore, they have been utilized more extensively in identifying plant diseases and pests.

It is rather remarkable that the wheat disease detection results from either spaceborne or airborne remotely sensed images must be validated by ground truth data. In the past several years, non-imaging field hyperspectral spectroeters such as ASD's spectrometers have been proved effective and reliable to evaluate the identification of diseases<sup>14</sup>. Nevertheless, they can only acquire mixed spectral information including stem, soil, shades, etc. for a disease-infected wheat canopy. It is therefore imperative that spectral purification techniques can emerge. Over the last several years, ground-based hyperspectral imaging spectrometers have been paid more attention to plant nutrient diagnosis and various crop stresses in precision agriculture<sup>15-20</sup>. However, few researches about wheat diseases were reported using the

ground-based hyperspectral imaging spectrometers. Considering the above issues and the characteristics of wheat leaves infected with powdery mildew symptoms, a domestic-made ground-based hyperspectral imaging spectrometer was utilized. This study is to characterize and identify powdery mildew of individual wheat leaves using techniques of spectral analysis in conjunction with image classification.

**Material and method**

**Hyperspectral Imaging System:** The hyperspectral imaging system used in this study is a ground-based pushbroom imaging spectrometer (PIS), which acquires images by linear array pushbroom imaging. It was jointly developed by Beijing Research Center for Information Technology in Agriculture and University of Science and Technology of China. This system includes four primary parts: a hyperspectral imaging spectrometer, lifting and lowering slide track, computer and hand control machine (Fig. 1). In a single scanning process, it can collect hyperspectral image cube and pixel-by-pixel spectral information within the wavelength range of 400-1,000 nm. Table 1 lists the key specification parameters of this system.

**Experimental design:** At the grain-filling stage of wheat, which was a key yield-forming period, an experiment was conducted in the wheat farm of Beijing Academy of Agriculture and Forestry Sciences (39.93° N, 116.27° E) on 26 May 2010. The tested winter wheat cultivar was Jingdong-12 under normal water and fertilizer-nitrogen management. In our experiment, seven groups of the top second wheat leaves with different severity levels were collected. To keep wheat leaves fresh, the PIS device was installed in a dark room near the experiment field. After wheat leaves were picked, they were fixed using some thumb tacks on the sampling platform covered with a black cloth (Fig. 1).

**Disease severity assessment:** Powdery mildew is characterized by a powdery white to gray fungal growth on wheat leaves, which can be recognized as fluffy white mold growth on leaf surfaces. When powdery mildew-infected symptoms of wheat leaves were evaluated, relative disease damage levels were estimated in accordance with the pathological criteria for the diagnosis of wheat powdery mildew. Consequently, according to the number and infestation area of disease spots for each leaf, four severity levels were classified: normal (there were not any disease spots), light (both the number and the area were small), moderate (the area was large but the number was small, or the area was small but the number was large) and serious (both the number and the area were large). Fig. 2 shows a visual comparison of different infestation levels at the leaf scale.

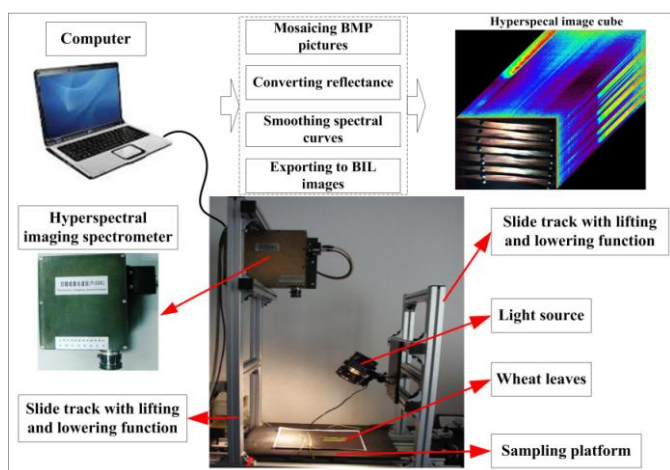


**Fig. 2: A visual comparison of different infestation levels at the leaf scale.**

**Fig. 1: Structural formation of the PIS and a demonstration of acquiring the spectra combing with image of wheat leaves infected with powdery mildew using the PIS.**

**Table 1**

**Key specification parameters of the PIS.**

Sensor parameters	Parameter values
Spectral range	400-1000 nm
Spectral resolution	2 nm
Sampling interval	0.7 nm
Field of View (FOV)	16°
Spatial resolution	5-10 mm
Pixel dimension	7.4 μm×7.4 μm
Image resolution	1400 (Spatial dimension) × 1024 (Spectral dimension)

**Data acquisition and preprocessing:** Before measuring wheat leaves, the height of lens of the PIS was fixed at 38 cm over the leaves according to the FOV of PIS. The machine moved at a speed of 24 mm/s considering the focal length and object distance and the halogen lamp irradiation was fixed at a 45° angle. Afterwards, each parameter set was performed in the control software and the lamp was opened. In accordance with corresponding setups, the hyperspectral image cubes were collected by the PIS (Fig. 1).

After acquiring the original hyperspectral images, they must be further processed. There were three primary steps: (1) hundreds of BMP format pictures were mosaiced to form an entire BIL format image in the Matlab programming environment; (2) reflectance conversion was carried out using an empirical linear method (eq. 1); (3) a moving-average smoothing algorithm was utilized to exclude abnormal values and smooth the spectral curves. The most important

aspect was that the little white reference panel must be used to optimize the instrument before and after collecting the spectra. To obtain the final spectral reflectance for each leaf, five region of interest (ROIs) were evenly selected to derive the mean spectrum from the tip to the bottom.

$$\rho = a * DN + b \tag{1}$$

where  $\rho$  is the real reflectance, a and b are the coefficients, DN (Digital Number) is the pixel value from original image. When putting the measured spectral value and corresponding DN into Eq. 1, a and b can be obtained by the least-square method (LSM) and then  $\rho$  can be correspondingly obtained.

### Results

**Image characteristics of wheat powdery mildew:** A group of wheat leaves with different infestation levels was randomly selected to describe the image characteristics. To generate a near-natural appearing composite image, a band combination of 680 (red), 550 (green) and 460 nm (blue) was

used. The acquired hyperspectral image showed a little dark, especially on the margin. The reason for this phenomenon was that non-uniform light irradiation was caused during the scanning process using single direction halogen lamps. To remove the influence of thumb tacks, a rectangle ROI was used to create a masked composite image (Fig. 3(a)). In order to analyze the differences of texture information between normal and powdery mildew-covered wheat leaves, occurrence-based filters were performed in the Environment for Visualizing Images (ENVI) image processing environment<sup>21</sup>. Consequently, five occurrence filters available of red band were obtained including data range, mean, variance, entropy and skewness (Fig. 3(b)). It could be found that the disease spots were obviously discernible in the images of mean, variance and data range, but conversely the available information was insufficient for the images of entropy and skewness. Therefore, a false composite image was formed using the images of mean, variance and data range (Fig. 3(c)). As shown in Fig. 3(c), there was obvious difference between normal leaf and disease spots. The disease spots of powdery mildew appeared in white color compared with green wheat leaves.

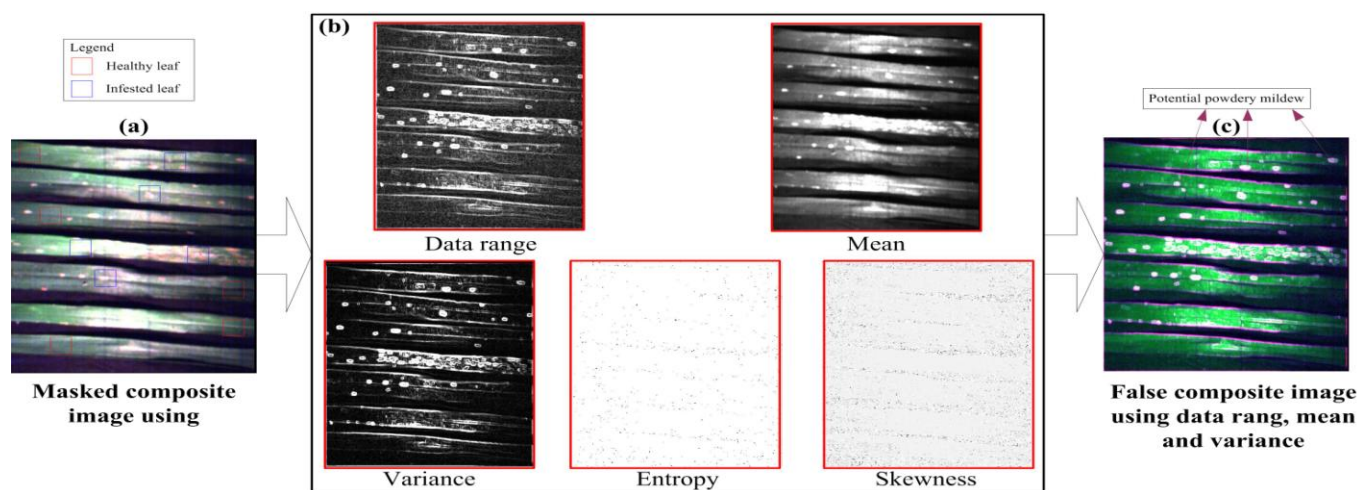


Fig. 3: Texture analysis of the high spatial resolution PIS image.

Based on every ten specified ROIs for normal and infested leaves (Fig. 3(a)), the corresponding statistical parameters of three texture filters were derived from the statistical functions of ENVI (Table 2). It could be found that all the statistical parameters of infested leaves were greater than that of normal leaves. The phenomenon could be interpreted that

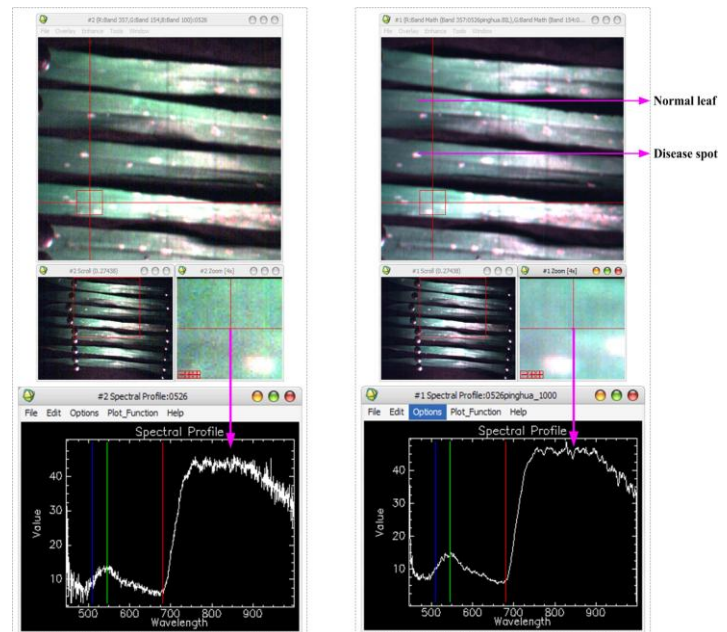
the cover of powdery mildew increased the sense of concavo-convex, so the texture information was richer than that of the relatively flat normal leaves. Considering the differences of three filters, the largest one was the maximum value of mean (23.300) and the smallest one was the minimum value of variance (0.006).

Table 2  
Statistical parameters of texture filters between normal and infested wheat leaves.

	Data range				Mean				Variance			
	Min	Max	Mean	Stdev	Min	Max	Mean	Stdev	Min	Max	Mean	Stdev
Normal leaves	0.174	1.130	0.584	0.164	2.664	4.807	3.864	0.397	0.004	0.124	0.035	0.018
Infested leaves	0.349	8.254	2.956	1.661	7.065	28.107	14.654	3.993	0.010	8.106	1.210	1.333
Difference*	0.175	7.124	2.372	1.497	4.401	23.300	10.790	3.596	0.006	7.982	1.175	1.315

\* shows that the values were derived from the subtraction of texture statistical parameters between normal and infested leaves.

**Spectral responses of different powdery mildew-infected levels:** To show the necessity of image smoothing, Fig. 4 demonstrated the comparison of hyperspectral curves between pre- and post-smooth. It was obvious that the hyperspectral curve was greatly smoothed, especially at the wavelengths of 445-680 and 760-1000 nm. Before comparing the spectral curves of four severity levels, two pixels with normal leaf and disease spot (Fig. 4) were selected to demonstrate their spectral differences (Fig. 5A). We could find that the reflectance of disease spot was greatly greater than that of normal leaf at the wavelength of 450-950 nm. The typical spectral characteristics (blue and red valleys, green peak) of leaf pixel covered with spot disease had lost in the visible spectrum. Therefore, a conclusion could be drawn that the reflectance of normal leaf was greatly enhanced due to the cover of powdery mildew spot disease. Furthermore, taking four leaves with normal, light, moderate and serious infestation levels for example, their spectral curves were comparatively analyzed. To clearly reflect the spectral characteristics for each level, their average reflectance values were obtained by averaging the ROIs along the entire leaf (Fig. 5B). It could be found that the reflectance increasingly increased with the increase of infestation severity.



**Fig. 4: A comparative of hyperspectral curves before and after smoothing the hyperspectral image cube.**

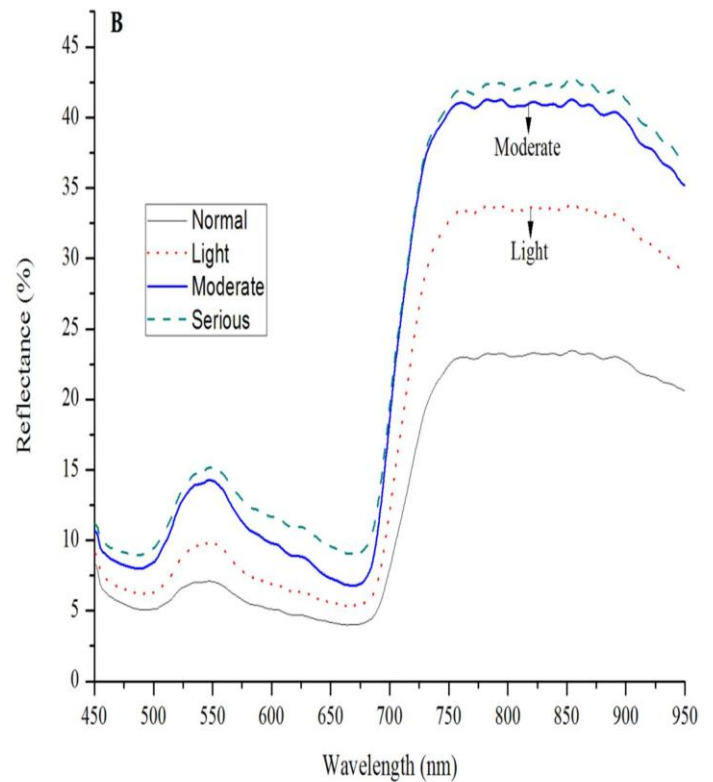
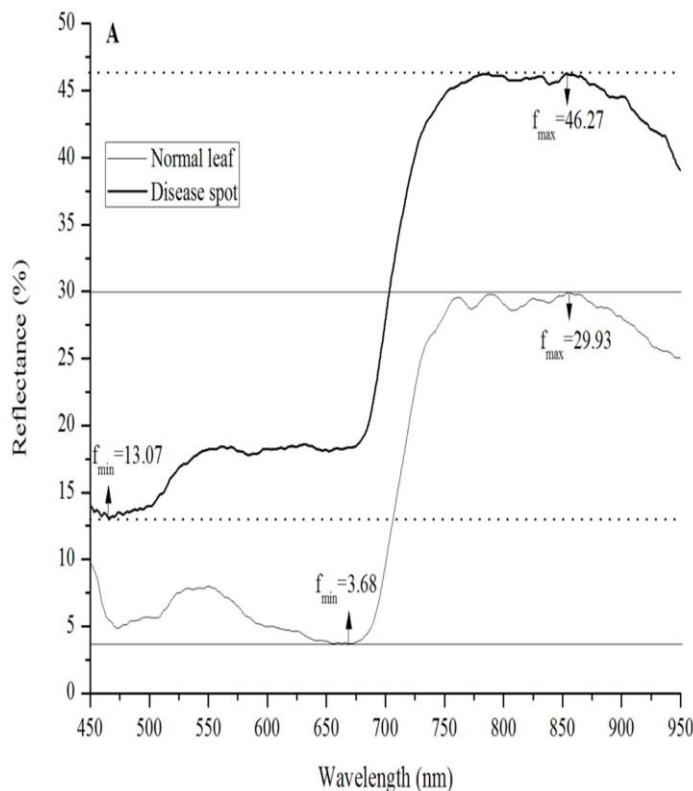


**Fig. 5: Hyperspectral curves derived from two pixels of normal leaf and spot disease (A) and four infestation levels (B).**

**Identification of powdery mildew at leaf scale:** In the high-resolution PIS image of wheat leaves, 110 pixels covered with powdery mildew and 110 pixels with normal leaf were selected at random. To find out the spectral characteristic bands with the largest spectral difference, a difference operation was performed between normal and powdery mildew-infected pixels in the wavelength of 450-950 nm.

According to the construction of normalized difference vegetation index (NDVI), red and near-infrared (NIR) spectral regions were considered as the two ranges sensitive to changes in the amount of green biomass and chlorophyll content<sup>22</sup>. In our study, two spectral sensitive bands were obtained by averaging the ten continuous bands with the largest spectral difference in the red and near-infrared wavelengths, respectively.

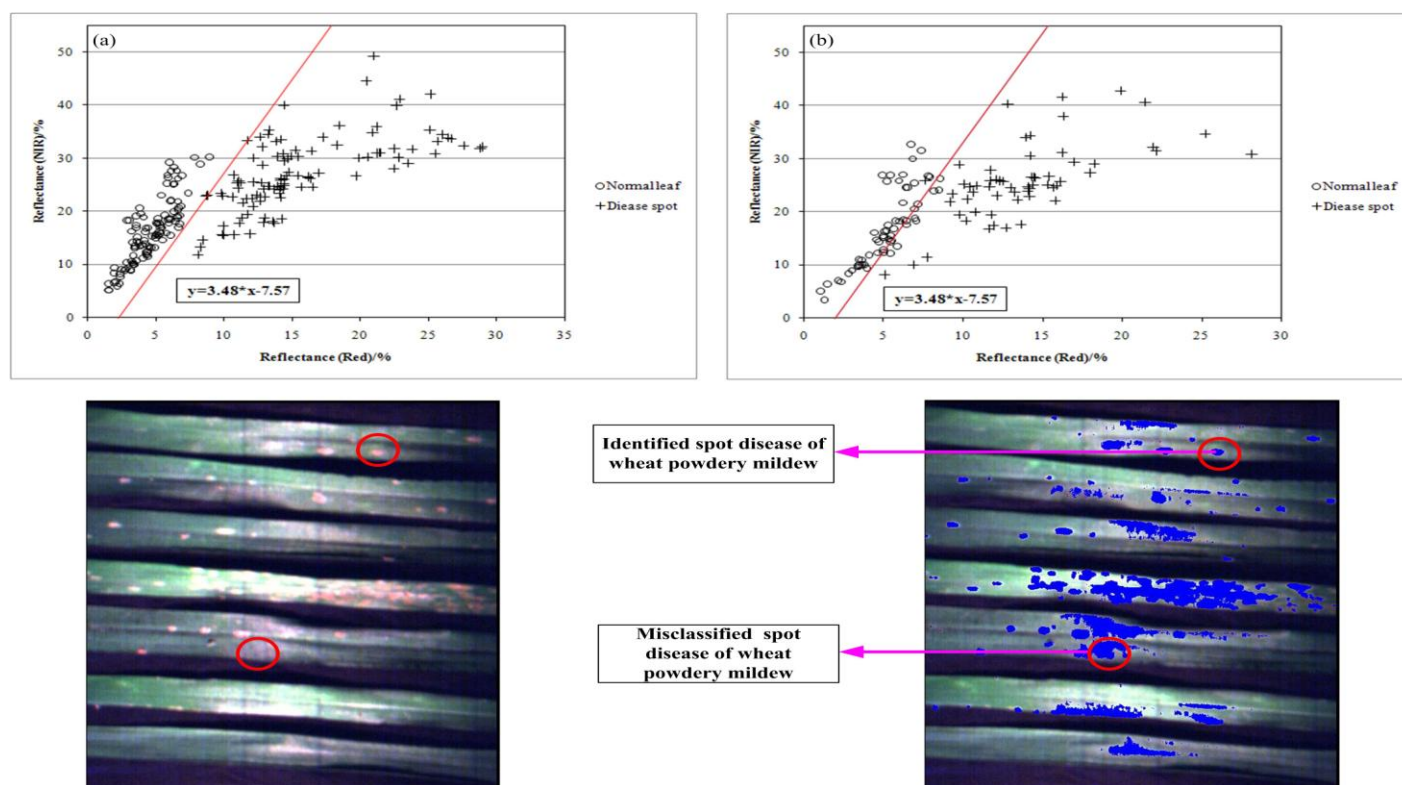


**Fig. 6: Identified disease spots of powdery mildew from normal wheat leaves.**

Consequently, 10 Red bands (675.1-681.1 nm) and 10 NIR bands (706.2-712.1 nm) were averaged and two average bands were used to build an image feature space (X axis: red; Y axis: NIR). In our study, a total of 220 pixels were averagely selected to construct the identification linear regression model for normal leaf and disease spot (Fig. 6(a)). It was obvious that the distribution of points of disease spots was more discrete than that of normal leaf. To validate the accuracy of this model, 60 pixels were selected for each level. The identification result showed that 8 pixels were misclassified as normal leaf and 1 pixel was misclassified as disease spot. Therefore, the overall classification accuracy reached 92.5%. As seen in the identified image (Fig. 6), most of disease spots were identified, but some pixels were obviously misclassified as disease spots from normal leaves because of the influence of non-uniform lighting.

**Conclusion and Discussion**

In this study, the image and spectral characteristics of wheat leaves infected with powdery mildew was fully analyzed using a near-ground hyperspectral imaging system. It has been proved that this system can be sufficiently used in identifying the wheat disease information. By building a linear regression model, disease spots were mostly identified. However, some misclassification was also caused due to non-uniform lighting in the process of scanning. In comparison with relatively flat leaves, pustular spots of powdery mildew increase the values in both texture and spectral information. Consequently, the abrupt changes lay a theoretical foundation for identifying disease using high spatial and spectral resolution hyperspectral data cubes acquired by the ground-based hyperspectral imaging spectrometer.

Nevertheless, with the increase of spectral bands, their data volume also increases greatly and more effective band compression algorithms will be required. In our study, it is comparatively easy to identify leaf-scale wheat disease due to single background. To identify wheat diseases more correctly at the canopy scale, a combination of texture and spectral information must be jointly utilized due to the influence of complex background in a field survey.

**Acknowledgement**

The project was supported by China Postdoctoral Science Foundation funded project (20110490317), National Natural Science Foundation of China (41071276, 41101395), Program of Ministry of Agriculture (200903010), Special Funds for Major State Basic Research Project (2007CB714406) and Postdoctoral Science Foundation of Beijing Academy of Agriculture and Forestry Sciences (2011).

**References**

1. Kuckenber J., Tartachnyk I. and Noga G., Detection and differentiation of nitrogen-deficiency, powdery mildew and leaf rust at wheat leaf and canopy level by laser-induced chlorophyll fluorescence, *Biosystem Engineering*, **103**(2), 121-128 (2009)
2. Murray G.M. and Brennan J.P., Estimating disease losses to the Australian wheat industry, *Australasian Plant Pathology*, **38** (6), 558-570 (2009)
3. Lan C.X. et al, Quantitative trait loci mapping of adult-plant resistance to powdery mildew in Chinese wheat cultivar Lumai 21, *Molecular Breeding*, **25**(4), 615-622 (2010)

4. Bravo C. et al, Early disease detection in wheat fields using spectral reflectance, *Biosystem Engineering*, **84(4)**, 137-145 (2003)
5. Yang Z. et al, Differentiating stress induced by greenbugs and Russian Wheat aphids in wheat using remote sensing, *Computers and Electronics in Agriculture*, **74(1)**, 64-70 (2009)
6. Rumpf T. et al, Early detection and classification of plant diseases with Support Vector Machines based on hyper spectral reflectance, *Computers and Electronics in Agriculture*, **74(1)**, 91-99 (2010)
7. Graeff S., Link J. and Claupein W., Identification of powdery mildew (*Erysiphe graminis* sp. *tritici*) and take-all disease (*Gaeumannomyces graminis* sp. *tritici*) in wheat (*Triticum aestivum* L.) by means of leaf reflectance measurements, *Central European Journal of Biology*, **1(2)**, 275-288 (2006)
8. Nicholas H., Using remote sensing to determine the date of a fungicide application on winter wheat, *Crop Protection*, **23(9)**, 853-863 (2004)
9. Franke J. and Menz G., Multi-temporal wheat disease detection by multi-spectral remote sensing, *Precision Agriculture*, **8(3)**, 161-172 (2007)
10. Chen X. et al, Detecting infestation of take-all disease in wheat using Landsat Thematic Mapper imagery, *International Journal of Remote Sensing*, **28(22)**, 5183-5189 (2007)
11. Li J. et al, Using hyperspectral indices to estimate foliar chlorophyll a concentrations of winter wheat under yellow rust stress, *New Zealand Journal of Agricultural Research*, **50(5)**, 1031-1036 (2007)
12. Mewes T., Franke J. and Menz G., Spectral requirements on airborne hyperspectral remote sensing data for wheat disease detection, *Precision Agriculture*, **12(6)**, 795-812 (2011)
13. Hatfield P.L. and Pinter P.J., Remote sensing for crop protection, *Crop Protection*, **12(6)**, 403-413 (1993)
14. Huang W.J. et al, Identification of yellow rust in wheat using in-situ spectral reflectance measurements and airborne hyperspectral imaging, *Precision Agriculture*, **8(4-5)**, 187-197 (2007)
15. Nilsson H.E., Hand-held radiometry and IR-thermography of plant diseases in field plot experiments, *International Journal of Remote Sensing*, **12(3)**, 545-557 (1991)
16. Inoue Y. and Penuelas J., An AOTF-based hyperspectral imaging system for field use in ecophysiological and agricultural applications, *International Journal of Remote Sensing*, **22(18)**, 3883-3888 (2001)
17. Fitzgerald G.J., Portable hyperspectral tunable imaging system (PHYTIS) for precision agriculture, *Agronomy journal*, **96(1)**, 311-315 (2004)
18. Moshou D. et al, Plant disease detection based on data fusion of hyper-spectral and multi-spectral fluorescence imaging using Kohonen maps, *RealTime Imaging*, **11(2)**, 75-83 (2005)
19. Ye X.J. et al, A ground-based hyperspectral imaging system for characterizing vegetation spectral features, *Computers and Electronics in Agriculture*, **63(1)**, 13-21 (2008)
20. Nansen C., Sidumo A.J. and Capareda S., Variogram analysis of hyperspectral data to characterize the impact of biotic and abiotic stress of maize plants and to estimate biofuel potential, *Applied Spectroscopy*, **64(6)**, 627-636 (2010)
21. Haralick R.M., Shanmugan K. and Dinstein I., Textural Features for Image Classification, *IEEE Transactions on Systems, Man and Cybernetics*, **3(6)**, 610-621 (1973)
22. Rouse J.W. et al, Monitoring vegetation systems in the great plains with ERTS, *Third NASA ERTS Symposium*, **1**, 309-317(1973).

(Received 02<sup>nd</sup> January 2012, accepted 10<sup>th</sup> June 2012)

\*\*\*\*\*